

Systematic $1/d$ Corrections to the Infinite-Dimensional Limit of Correlated Lattice Electron Models

Avraham Schiller* and Kevin Ingersent*

Department of Physics, University of Florida, 215 Williamson Hall, Gainesville, Florida 32611

(Received 6 March 1995)

We present a self-consistent treatment of Hubbard-like lattice models at large, but finite, spatial dimensions d . This involves a systematic expansion in powers of $1/d$ about the limit $d = \infty$. The first-order corrections can be obtained by self-consistent solution of coupled one- and two-impurity models. We calculate the leading corrections to properties of the Falicov-Kimball model. The infinite-dimensional limit seems to describe this particular model remarkably well even for $d = 2$.

PACS numbers: 71.27.+a, 71.45.Lr, 75.10.Lp, 75.30.Fv

The limit of large spatial dimensions d [1] has been used extensively to study models of correlated lattice fermions [2]. The local approximation, which maps a lattice problem onto a single-impurity model supplemented by a self-consistency condition that simulates the role of the lattice, is exact at $d = \infty$ [3]. This provides a dynamical mean-field theory which captures much of the rich physics of correlated lattice models [4–7]. The local approximation cannot, however, address the existence of instabilities towards unconventional superconductivity [4], or fully probe the competition between correlation and magnetism in heavy-fermion compounds. To date, attempts to recover the effects of spatial fluctuations through systematic expansion about the limit $d = \infty$ have succeeded only in a few special cases: the Gutzwiller variational approach [8], the motion of a single hole in the $J = 0$ t - J model [9], and the spinless-fermion model [10]. Extension to the Hubbard Hamiltonian and related models, containing full many-body effects, has proved elusive.

In this paper we present a systematic theory of $1/d$ corrections for all Hubbard-like models, in the form of an effective cluster expansion. At leading order in $1/d$, the local approximation is replaced by a mapping onto coupled single- and two-impurity models. As a first step towards implementing this theory, we have explicitly obtained leading $1/d$ corrections for the Falicov-Kimball Hamiltonian, a restricted model to which a simplified version of this method can be applied. Only small deviations are found from the local approximation, even for $d = 2$. For larger values of the on-site Coulomb interaction, nonanalyticities develop within the simplified scheme. We expect $1/d$ corrections to have a much greater effect in the Hubbard and periodic Anderson Hamiltonians, models which are more relevant for the issues mentioned above.

We take as our generic model the Hubbard Hamiltonian on a d -dimensional hypercubic lattice

$$\mathcal{H} = -\frac{t^*}{\sqrt{d}} \sum_{\langle i,j \rangle, \sigma} c_{i\sigma}^\dagger c_{j\sigma} + U \sum_i n_{i\uparrow} n_{i\downarrow}. \quad (1)$$

Here the nearest-neighbor hopping is scaled so that the kinetic energy has a suitable $d \rightarrow \infty$ limit. This implies

[1,11] that in real space the bare ($U = 0$) propagator $G_{ij\sigma}^{(0)}$ is proportional to $d^{-\|i-j\|/2}$, where $\|i-j\|$ is the smallest number of nearest-neighbor hops between sites i and j . To leading order, the fully dressed single-particle lattice Green's function $G_{ij\sigma}$ has the same d dependence.

A concise formulation of $1/d$ corrections employs the Luttinger-Ward functional $\Phi[G_{ij\sigma}]$ —the sum of all vacuum-to-vacuum skeleton diagrams—in terms of which the self-energy is

$$\Sigma_{ij\sigma}(i\omega_n) = \frac{\delta\Phi}{\delta G_{ji\sigma}(i\omega_n)}. \quad (2)$$

Any two vertices i and j within a closed skeleton diagram can be connected by four paths having no line in common. For example, the diagram in Fig. 1 contains two paths going directly from i to j , and two going via site k . After summation over intermediate sites, each path contributes to a given diagram at least the same power of $1/d$ as $G_{ij\sigma}$. Even after summation over all equivalent sites j , the diagram is suppressed by a factor of at least $1/d^{\max}$, where \max is the greatest intersite distance in that diagram. Thus, to order $1/d^n$, all diagrams containing intersite distances greater than n are negligible. This has two consequences for the self-energies: by virtue of Eq. (2),

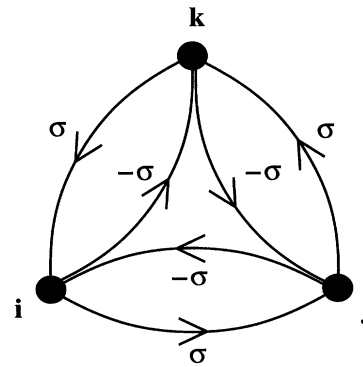


FIG. 1. A typical diagram in the expansion of the Luttinger-Ward functional, $\Phi[G_{ij\sigma}]$. Lines represent fully dressed Green's functions, circles indicate on-site Coulomb interactions.

one need consider only those $\Sigma_{ij\sigma}$ with $\|i - j\| \leq n$; furthermore, the remaining self-energies reduce to functionals solely of $G_{kl\sigma}$ with $\|k - l\| \leq n$. Hence, *summation of all skeleton diagrams with no intersite distance greater than n constitutes a systematic approximation scheme correct to order $1/d^n$* . An equivalent classification can be deduced directly from the diagrammatic representation of the self-energies [12].

Let us focus on first-order corrections in $1/d$. Then, Φ reduces to all possible skeleton diagrams that are either purely local, or involve just a *single* pair of nearest-

neighbor sites. Consequently, we can write

$$\Phi[G] = \sum_{\langle i,j \rangle, \sigma} \Phi_{2\text{-imp}}[G_{ii\sigma}, G_{ij\sigma}, G_{ji\sigma}, G_{jj\sigma}] - (2d - 1) \sum_{i,\sigma} \Phi_{1\text{-imp}}[G_{ii\sigma}], \quad (3)$$

where $\Phi_{1\text{-imp}}$ and $\Phi_{2\text{-imp}}$ are the generating functionals for one and two Hubbard impurities, respectively. The second term in Eq. (3) prevents overcounting of purely local diagrams. $\Phi_{1\text{-imp}}$ and $\Phi_{2\text{-imp}}$, respectively, can be generated from the one- and two-impurity actions

$$S_{1\text{-imp}} = - \int_0^\beta d\tau \int_0^\beta d\tau' \sum_{\sigma} c_{1\sigma}^\dagger(\tau) \mathcal{G}_{1\text{-imp},\sigma}^{(0)-1}(\tau - \tau') c_{1\sigma}(\tau') + U \int_0^\beta d\tau c_{1\uparrow}^\dagger(\tau) c_{1\uparrow}(\tau) c_{1\downarrow}^\dagger(\tau) c_{1\downarrow}(\tau), \quad (4a)$$

$$S_{2\text{-imp}} = - \int_0^\beta d\tau \int_0^\beta d\tau' \sum_{i,j=1}^2 \sum_{\sigma} c_{i\sigma}^\dagger(\tau) [\mathcal{G}_{2\text{-imp},\sigma}^{(0)-1}(\tau - \tau')]_{ij} c_{j\sigma}(\tau') + U \sum_{i=1}^2 \int_0^\beta d\tau c_{i\uparrow}^\dagger(\tau) c_{i\uparrow}(\tau) c_{i\downarrow}^\dagger(\tau) c_{i\downarrow}(\tau). \quad (4b)$$

The site indices 1 and 2 label a specific pair of nearest-neighbor lattice sites. $\mathcal{G}_{1\text{-imp},\sigma}^{(0)}(\tau - \tau')$ and $\mathcal{G}_{2\text{-imp},\sigma}^{(0)}(\tau - \tau')$, the latter being a 2×2 matrix, represent the “bare” propagators. These are to be chosen so that, when dressed with the impurity self-energies, they coincide with the corresponding lattice Green’s functions

$$\mathcal{G}_{1\text{-imp},\sigma}^{(0)-1}(i\omega_n) = G_{11\sigma}^{-1}(i\omega_n) + \Sigma_{\sigma}^{1\text{-imp}}(i\omega_n), \quad (5a)$$

$$[\mathcal{G}_{2\text{-imp},\sigma}^{(0)-1}(i\omega_n)] = [G_{\sigma}^{-1}(i\omega_n)]_{ij} + \Sigma_{ij\sigma}^{2\text{-imp}}(i\omega_n). \quad (5b)$$

Here our 2×2 matrix notation has been extended to G_{σ} , i.e., $[G_{\sigma}(i\omega_n)]_{ij} \equiv G_{ij\sigma}(i\omega_n)$.

Solution of the impurity problems allows one to extract the impurity self-energies from the lattice propagators. Then a functional derivative of Eq. (3) relates the lattice and impurity self-energies. In the paramagnetic phase all spin dependence drops out and just two lattice self-energies remain: the on-site $\Sigma_0(z)$ and nearest-neighbor $\Sigma_1(z)$ self-energies. These can be written

$$\Sigma_0(i\omega_n) = \Sigma^{1\text{-imp}}(i\omega_n) + 2d \left[\Sigma_{11}^{2\text{-imp}}(i\omega_n) - \Sigma^{1\text{-imp}}(i\omega_n) \right], \quad (6a)$$

$$\Sigma_1(i\omega_n) = \Sigma_{11}^{2\text{-imp}}(i\omega_n). \quad (6b)$$

Similar relations hold for phases with long-range order.

A self-consistent loop can be closed by expressing the full Green’s functions in terms of the lattice self-energies. This relation will depend on the specific phase under consideration. For the spatially homogeneous phase, solution of the lattice Dyson’s equation yields

$$G_{ij\sigma}(z) = \frac{1}{1 + \Sigma_1(z)/t} G_{ij\sigma}^{(0)} \left(\frac{z - \Sigma_0(z) + \mu}{1 + \Sigma_1(z)/t} \right). \quad (7)$$

The bare $G_{ij\sigma}^{(0)}$ functions (corresponding to a chemical potential $\mu = 0$) must be taken to be the actual d -dimensional propagators, or unphysical results will emerge. This is because on a hypercubic lattice, the

bare propagators have nonanalytic corrections in $1/d$ that cannot be treated within perturbation theory in $1/d$ [11]. The self-consistency requirement is enforced numerically according to the following iteration scheme:

$$\Sigma^{\text{imp}} \xrightarrow{\text{Eqs. (6)}} \Sigma^{\text{latt}} \xrightarrow{\text{Eq. (7)}} G^{\text{latt}} \xrightarrow{\text{Eqs. (5)}} \mathcal{G}_{\text{imp}}^{(0)} \xrightarrow{\text{Solve imp. actions}} \Sigma^{\text{imp}}. \quad (8)$$

The above constitutes a self-consistent theory, correct to order $1/d$, which by construction is thermodynamically conserving. It can be extended to describe phases with long-range order, as well as other related models [12]. An equivalent theory has been formulated independently by Georges and Kotliar [13].

Among the steps entering Eq. (8), solution of the impurity actions is by far the most complicated, since it requires the solution of one- and two-impurity Anderson-like models. Application of the above formulation of $1/d$ corrections to any correlated lattice model therefore requires a large-scale numerical effort. In what follows we focus on the Falicov-Kimball model, for which a simplified version of the $1/d$ treatment can be implemented.

In the Falicov-Kimball Hamiltonian [14],

$$\mathcal{H} = - \frac{t^*}{\sqrt{d}} \sum_{\langle i,j \rangle} d_i^\dagger d_j + E_f \sum_i f_i^\dagger f_i + U \sum_i f_i^\dagger f_i d_i^\dagger d_i, \quad (9)$$

itinerant d fermions interact with localized f fermions via an on-site Coulomb interaction U . (This can be regarded as a variant of the Hubbard model in which one spin species is tied down.) The two fermion species share a joint chemical potential μ and are thermodynamically correlated, leading to long-range ordered phases. Most notably, in the symmetric case $E_f = 0$, $\mu = U/2$, a checkerboard decomposition of the f particles occurs, with a finite critical temperature T_c for any $d \geq 2$ [15].

The localized nature of the f fermions in the Falicov-Kimball model permits a greatly simplified treatment of

$1/d$ corrections. Expanding in terms of fully dressed d propagators and bare f propagators, we can still obtain a classification in powers of $1/d$ based on the greatest intersite distance within a diagram, and hence derive impurity mappings similar to Eqs. (4). Now, however, just as for $d = \infty$ [16], bare f propagators enter the

$$\mathcal{G}_{1\text{-imp}}(i\omega_n) = \sum_{\gamma=0,1} w_\gamma [\mathcal{G}_{1\text{-imp}}^{(0)-1}(i\omega_n) - \gamma U]^{-1}, \quad (10a)$$

$$\mathcal{G}_{2\text{-imp}}(i\omega_n) = \sum_{\gamma,\delta=0,1} p_{\gamma\delta} \left[\mathcal{G}_{2\text{-imp}}^{(0)-1}(i\omega_n) - U \begin{pmatrix} \gamma & 0 \\ 0 & \delta \end{pmatrix} \right]^{-1}. \quad (10b)$$

Here γ and δ represent the f -occupancy number on sites 1 and 2, respectively; w_γ and $p_{\gamma\delta}$ are probabilities for the different f configurations in each impurity action. Different Matsubara frequencies $i\omega_n = i(2n+1)T$ are coupled only through the probabilities, which are expressed as sums over all $i\omega_n$ [16]. Apart from this, Eqs. (10) implement the impurity-solution step of Eq. (8) in a purely algebraic manner. Once Eq. (8) has been iterated and the probabilities w_γ and $p_{\gamma\delta}$ determined, the same sequence can be used to calculate $G_{ij}(z)$ for an arbitrary complex z . A special feature of the resulting equations is that they are purely local in z .

Although this simplified treatment is correct to order $1/d$, it is no longer thermodynamically conserving. It also neglects certain diagrams retained within the general scheme. For example, the f self-energy diagram in Fig. 2 is formally $O(1/d^2)$, yet it enters the general treatment at order $1/d$ since the part containing site k can be absorbed into a dressed f propagator. By contrast, the d self-energy diagram obtained by swapping f and d

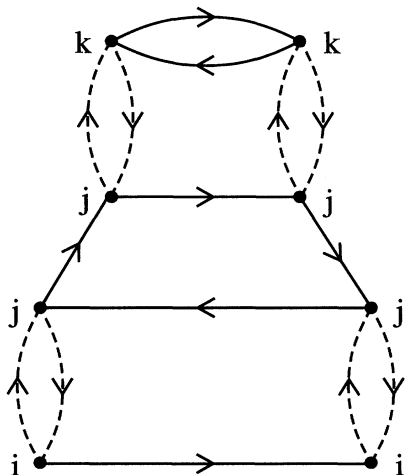


FIG. 2. An f self-energy diagram for the Falicov-Kimball model which is included in the general treatment of $1/d$ corrections but is omitted under the simplified scheme. Solid and dashed lines represent bare f and d propagators, respectively. Sites i and k are distinct nearest neighbors of j . There is summation over j and k for fixed i .

impurity actions, and the self-consistency equation applies only to the d propagators. As an important consequence, solution of the impurity actions no longer requires heavy computation. The d -fermion lattice Green's function $G_{ij}(z)$ is calculated by integrating out the f particles and expressing the one- and two-impurity d propagators as

lines in Fig. 2 enters both formulations at first order. The simplified scheme thus treats d and f fermions on different footings. This also leads to the locality in z of Eqs. (10).

We believe that this locality is responsible for the appearance of unphysical solutions to Eqs. (8). Let us focus on the spatially homogeneous phase ($T > T_c$) of the symmetric model ($E_f = 0$, $\mu = U/2$). As U exceeds a critical value U_c ($\approx 1.85t^*$ for $d = 2$), a patch develops around $z = 0$ —growing with increasing U —within which two distinct solutions for $G_{ij}(z)$ can be found. Both solutions are nonanalytic along the real axis: they violate the spectral sum rule and the Kramers-Kronig relation, although the spectral function remains non-negative. Analyticity is restored for z well above the real axis. We note that similar difficulties were encountered in attempts to go beyond the single-site mapping (coherent potential approximation) for disordered systems [17].

We concentrate on $U < U_c$, for which one can confirm numerically that the single solution that emerges is Herglotz: it fulfills both the spectral sum rule and the constraints of the spectral representation, and shows the correct asymptotic behavior $G_{ii}(z) \sim 1/z$ for $|z| \rightarrow \infty$. Figure 3 depicts the itinerant density of states in the homogeneous phase of the symmetric Falicov-Kimball

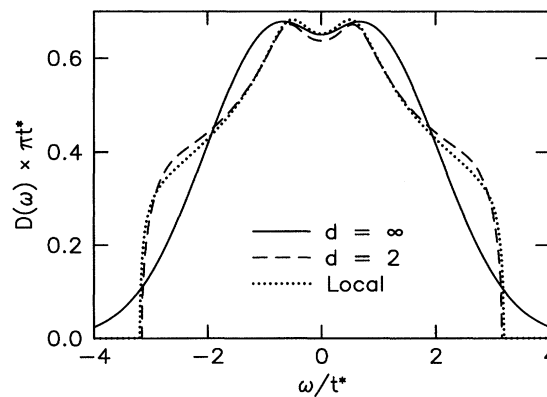


FIG. 3. The density of states for itinerant d fermions in the symmetric Falicov-Kimball model, with $U/t^* = 1.5$ and $T/t^* = 0.1$. The dotted line corresponds to the local approximation for $d = 2$.

model for $d = 2, \infty$, with $U/t^* = 1.5$ and $T/t^* = 0.1$. The results of the local approximation—a single-impurity mapping, using the true d dependence of $G_{ij}^{(0)}$ —are shown for comparison. Deviations from the local approximation practically vanish for $U/t^* \lesssim 1$. This is to be expected, at least in weak coupling, since corrections to the local approximation appear first at order U^4 for the Falicov-Kimball model (compared to only U^2 for the Hubbard model). It is somewhat surprising, however, that the deviations remain so small even for $U/t^* = 1.5$.

The checkerboard decomposition of the symmetric Falicov-Kimball model can be treated using three effective impurity actions: a two-impurity action, and separate one-impurity actions for the inequivalent sublattices A and B . One must determine five self-energies ($\Sigma_A^{1\text{-imp}}$, $\Sigma_B^{1\text{-imp}}$, $\Sigma_{AA}^{2\text{-imp}}$, $\Sigma_{BB}^{2\text{-imp}}$, and $\Sigma_{AB}^{2\text{-imp}} \equiv \Sigma_{BA}^{2\text{-imp}}$) plus independent probabilities $w_{A\gamma}$ and $w_{B\gamma}$ for the one-impurity f configurations on the two sublattices. The critical temperature T_c is the highest temperature at which a broken-symmetry solution $w_{A\gamma} \neq w_{B\gamma}$ appears.

Figure 4 plots T_c versus U for $d = 2$ and ∞ . Within the range of U shown, Herglotz solutions for G_{ij} can be found both above and below the transition temperature (although multiple solutions may develop once T is lowered deep into the broken-symmetry phase). Deviations from the $d = \infty$ curve are remarkably small for $d = 2$. However, the effect of $1/d$ corrections is always to depress T_c relative to the local approximation, as is characteristic of fluctuations about a mean-field theory.

We expect $1/d$ corrections to be more significant for fully interacting models in which a small many-body energy scale appears at $d = \infty$ in addition to the bare scales in the Hamiltonian. For instance, since the Hubbard model maps onto one- and two-impurity Anderson models, the solution must reflect a competition between an on-site Kondo effect and an intersite RKKY

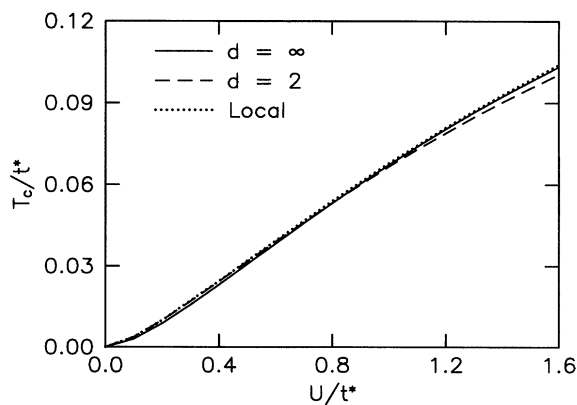


FIG. 4. The critical temperature for the checkerboard decomposition of the symmetric Falicov-Kimball model versus the strength of the Coulomb interaction. The dotted line shows the local approximation for $d = 2$.

interaction. This should capture the interesting physics that is missed at $d = \infty$.

In summary, we have presented a self-consistent expansion about the limit of infinite spatial dimensions for all Hubbard-like models. Implementation of leading-order $1/d$ corrections within a simplified scheme, specific to the Falicov-Kimball model, reveals nonanalytic Green's functions above some critical value of U . Below this value, solutions are Herglotz for all $T > T_c$ and into the broken-symmetry phase. Even for $d = 2$, the properties of the symmetric Falicov-Kimball model are modified only slightly, compared to the local approximation. It remains to be seen whether the appearance of multiple solutions is removed within the full expansion scheme.

We thank A. Georges and G. Kotliar for discussing their work with us prior to publication. This work was supported in part by the National Science Foundation, through the National High Magnetic Field Laboratory and Contract No. DMR-9316587.

*Affiliated with the National High Magnetic Field Laboratory, Tallahassee, Florida 32306.

- [1] W. Metzner and D. Vollhardt, Phys. Rev. Lett. **62**, 324 (1989).
- [2] See, e.g., D. Vollhardt, in *Correlated Electron Systems*, edited by V. J. Emery (World Scientific, Singapore, 1993).
- [3] For a comprehensive discussion, see A. Georges, G. Kotliar, and Q. Si, Int. J. Mod. Phys. B **6**, 705 (1992).
- [4] M. Jarrell, Phys. Rev. Lett. **69**, 168 (1992); M. Jarrell and Th. Pruschke, Z. Phys. B **90**, 187 (1993).
- [5] M. J. Rozenberg, X. Y. Zhang, and G. Kotliar, Phys. Rev. Lett. **69**, 1236 (1992); X. Y. Zhang, M. J. Rozenberg, and G. Kotliar, *ibid.* **70**, 1666 (1993).
- [6] A. Georges and W. Krauth, Phys. Rev. Lett. **69**, 1240 (1992).
- [7] J. K. Freericks, M. Jarrell, and D. J. Scalapino, Phys. Rev. B **48**, 6302 (1993).
- [8] W. Metzner, Z. Phys. B **77**, 253 (1989); **82**, 183 (1991); F. Gebhard, Phys. Rev. B **41**, 9452 (1990).
- [9] R. Strack and D. Vollhardt, Phys. Rev. B **46**, 13852 (1992).
- [10] E. Halvorsen, G. S. Uhrig, and G. Czycholl, Z. Phys. B **94**, 291 (1994).
- [11] E. Müller-Hartmann, Z. Phys. B **74**, 507 (1989).
- [12] A. Schiller and K. Ingersent (unpublished).
- [13] A. Georges and G. Kotliar (to be published).
- [14] L. M. Falicov and J. C. Kimball, Phys. Rev. Lett. **22**, 997 (1969).
- [15] U. Brandt and R. Schmidt, Z. Phys. B **63**, 45 (1986); **67**, 43 (1987); E. H. Lieb and T. Kennedy, Physica (Amsterdam) **138A**, 320 (1986); E. H. Lieb, *ibid.* **140A**, 240 (1986).
- [16] U. Brandt and C. Mielsch, Z. Phys. B **75**, 365 (1989); **79**, 295 (1990); **82**, 37 (1991); U. Brandt and M. P. Urbanek, *ibid.* **89**, 297 (1992).
- [17] For a review, see, e.g., R. J. Elliott, J. A. Krumhansl, and P. L. Leath, Rev. Mod. Phys. **46**, 465 (1974).